Journal of Cellular Physiology

RAGE Recycles at the Plasma Membrane in S100B Secretory Vesicles and Promotes Schwann Cells Morphological Changes

LORENA PERRONE,[1,2]* GIANFRANCO PELUSO,[3] AND MARIAROSA AB MELONE[4]

[1]*Department of Neurology, University of Michigan, Ann Arbor, Michigan*

[2]*Department of Anatomy and Cell Biology, Wayne State University, Detroit, Michigan*

[3]*Institute of Protein Biochemistry, IBP-CNR, Naples, Italy*

[4]*Department of Neurological Sciences, Second University of Naples, Naples, Italy*

RAGE is a multiligand receptor of the immunoglobulin superfamily involved in regeneration of injured peripheral nerve and cell motility. RAGE is implicated in the development of various chronic diseases, such as neurodegenerative disorders, inflammatory responses, and diabetic complications. The correlation between RAGE endocytic trafficking and RAGE function is still uninvestigated. S100B is one of the ligands of RAGE. The molecular mechanisms responsible of S100B translocation in exocytic vesicles are still poorly investigated. In the present study we elucidate the role of RAGE endocytic trafficking in promoting S100B secretion in Schwann cells. Here we show that RAGE-induced secretion of S100B requires phosphorylated caveolin1-dependent endocytosis of RAGE. Endocytosis of RAGE in response to ligand binding promotes the fusion of endosomes with S100B-positive secretory vesicles. Src promotes the fusion of endosomes with S100B-secretory vesicles. Inhibition of src induces RAGE degradation. RAGE-mediated src activation induces cav1 phosphorylation and relocalization in the perinuclear compartment. RAGE signaling and recycling are required for S100-induced Schwann cells morphological changes and are inhibited by high-glucose, suggesting a possible link between diabetes and peripheral nerve injury. Indeed, high glucose inhibits RAGE-mediated src activation. Src inhibition blocks RAGE recycling, S100B secretion, and morphological changes. In summary, we identified a novel pathway of vesicular trafficking required for the amplification of RAGE signaling and cytoskeleton dynamics that is potentially involved in the regeneration of injured peripheral nerve.

J. Cell. Physiol. 217: 60–71, 2008.

RAGE is a multiligand receptor of the immunoglobulin superfamily of cell surface molecules. RAGE ligands include AGEs, S100/calgranulins, HMGB1, amyloid-β peptides, and the family of β-sheets fibrils (Bierhaus et al., 2005). Amplification of RAGE-mediated signaling is implicated in the development of such chronic diseases as neurodegenerative disorders, inflammatory responses, and diabetic complications (Bierhaus et al., 2005; Vincent et al., 2007). RAGE also exerts physiological functions and its activity is required during regeneration of injured peripheral nerves (Rong et al., 2004a,b). Schwann cells (SC) are involved in the repair of nerve fibers (Dobrowsky et al., 2005) and in diabetic neuropathy (Kalichman et al., 1998). However, thus far, no study has addressed RAGE-mediated function in SC.

Although several studies have analyzed RAGE–mediated signaling (Bierhaus et al., 2005), the link between RAGE activation and RAGE endocytic trafficking has been poorly investigated. There is just one study showing that interaction of the amyloid-β peptide (Aβ) with RAGE in vascular endothelial cells leads to transport of Aβ across the blood-brain barrier thereby inducing the expression of pro-inflammatory cytokines (Deane et al., 2003).

The members of the S100 protein family lack the classical signal sequence for secretion. Thus, different S100 proteins use distinct translocation pathways. Translocation of S100B in vesicles plays an important role in the assembly of signaling complexes that activate specific signaling pathways (Davey et al., 2001). Interestingly, S100B relocates from cytosol to vesicles and induces cell motility (Mbele et al., 2002). However, the molecular mechanisms responsible for S100B translocation in vesicles have yet to be completely elucidated.

Recent studies have examined the role of RAGE in cell migration (Reddy et al., 2006; Riuzzi et al., 2006; Chavakis et al., 2007; Dumitriu et al., 2007; Orlova et al., 2007; Yang et al., 2007) and in the dynamics of actin cytoskeleton (Dumitriu et al., 2007). Both cell migration and changes in cell morphology require actin polymerization together with focal adhesion

This article includes Supplementary Material available from the authors upon request or via the Internet at http://www.interscience.wiley.com/jpages/0021-9541/suppmat.

Abbreviations: AGE, advanced glycation endproducts; RAGE, receptor of advanced glycation endproducts; HMGB1, high mobility group B1; IP, immunoprecipitate; PBS, phosphate buffered saline; TX-100, Triton X-100; PFA, parafolmaldeide; BSA, bovine serum albumin; dyn2, dynamin 2; PP1, pyrazolo pyrimidine-type inhibitor 1; PBS-CM, PBS solution containing 1.8 mM Ca^{2+} and 0.5 mM Mg^{2+}; rt, room temperature; HG, high glucose; LG, low glucose; EGF, endothelial growth factor.

Contract grant sponsor: NIH5P60, National Institute of Diabetes & Digestive & Kidney Diseases.
Contract grant number: N. DK20572.

*Correspondence to: Lorena Perrone, Department of Anatomy and Cell Biology, Wayne State University, 540 E. Canfield, 8336 Scott Hall, Detroit, MI. E-mail: lperrone@med.wayne.edu

Received 10 December 2007; Accepted 14 March 2008

DOI: 10.1002/jcp.21474

assembly and disassembly (Kruchten and McNiven, 2006). Dynamins exert a key function in modulating the dynamics of adhesion during migration and morphological changes, and dynamin is implicated in both clathrin-coated pits-mediated and caveolae-mediated endocytosis (Kruchten and McNiven, 2006). Phosphorylation and dephosphorylation of focal adhesion kinase (Fak) is important for the turnover of focal adhesion and subsequent reorganization of the actin cytoskeleton necessary for cellular movement (Kruchten and McNiven, 2006). By interacting with Fak, dyn2 is necessary for focal adhesion turnover (Kruchten and McNiven, 2006). Cytoskeletal and morphological changes are important for SC differentiation, which leads to myelinization of nervous fibers (Berti et al., 2006).

Given the relevance of endocytic trafficking in the receptor-mediated response, the role of RAGE and SC in the repair of injured nerves and in the development of neuropathy, and the lack of studies in these areas, we examined the endocytic trafficking of RAGE in SC. We demonstrate that endocytosis of RAGE in response to ligand binding promotes the fusion of endosomes with S100B-positive secretory vesicles. Fusion of endosomes with S100B-secretory vesicles is regulated by src. RAGE activation leads also to translocation of phosphorylated cav1 in the perinuclear compartment, where it co-localizes with dyn. We also show that RAGE triggering induces Fak activation and SC morphological changes. Interestingly, RAGE-induced src activation and SC morphological changes are inhibited by high glucose (HG) concentrations, thereby suggesting a molecular mechanism whereby the repair of injured nerves is delayed in diabetes.

Materials and Methods

Reagents

Cell culture reagents were purchased from GIBCO BRL (Invitrogen Corporation, Carlsbad, CA). NHS-LC-biotin, NHS-SS-biotin, Neutravidin beads, and HRP-linked streptavidin were from Pierce Chemical Co. (Rockford, IL). Biotin-conjugated anti rabbit IgG, methyl-β-cyclodestrin, glutathione, and all other reagents, unless otherwise stated, were purchased from Sigma–Aldrich (St. Louis, MI). Anti-RAGE-blocking antibody, which blocks receptor-ligand interaction, was from RD System (Minneapolis, MN, catalog number: AF1179). The src-specific inhibitor pyrazolo pyrimidine-type inhibitor 1 (PP1) (Schindler et al., 1999) was from Biomol (Plymouth Meeting, PA). S100 isolated from bovine brain, was obtained from Calbiochem (EMD Biosciences, San Diego, CA, catalog number: 559284).

Biotinylation assay and biotin internalization assay

Primary SC were isolated from sciatic nerves of 3-day-old Harlan Sprague–Dawley rats and cultured as described previously (Mikol et al., 2002). The advantage of these cells is that they can be frozen and re-cultured without losing their phenotype. Indeed, these cells do not develop replicative senescence during culturing (Mathon et al., 2001). Two different preparations were used for the experiments described. Various aliquots from two different preparations were de-frozen and cultured until passage 5. Twenty-four hours before stimulation with S100 (20 $\mu g\,ml^{-1}$), cells were serum-starved in Schwann cell-defined medium (SCDM) (50% DMEM, 50% Ham's F12, 10 $\mu g\,ml^{-1}$ transferrin, 10 μM putrescine, 20 nM progesterone, 30 nM sodium selenite). To investigate the half-life of surface RAGE, cells were biotinylated with NHS-LC biotin and processed as described previously (Zurzolo et al., 1993; Perrone et al., 2005). After biotinylation, cells were stimulated at 37°C with bovine brain-derived S100, a well-defined activator of RAGE (Hofmann et al., 1999; Vincent et al., 2007). Cells were lysed in RIPA buffer. Biotinylated antigens were pull-down with streptavidin-agarose beads. After boiling the beads in Laemmli buffer, supernatants were analyzed by SDS–PAGE and fluorography with preflashed films. To control the total amount of RAGE, 1/10 of the supernatant was analyzed by Western blotting. Densitometry was carried out within the linear range of the films.

For endocytosis assay, cells were biotinylated using cleavable biotin: sulphosuccinimidyl-6-(biotinamide) hexanoate (NHS-SS-biotin) as described elsewhere (Perrone et al., 2005). Samples were incubated at 37°C for different times in the presence of bovine brain S100, whereas control filters were kept at 4°C. After incubation, cells were lysed in RIPA buffer (10 mM Tris/Cl pH 8, 1% TX-100, 0.1% DOC, 0.1% SDS, 140 mM NaCl, and 1 mM PMSF). Biotinylated antigens were pulled-down with streptavidin-agarose beads. After the beads were boiled in Laemmli buffer, supernatants were analyzed by SDS–PAGE and fluorography with preflashed films. To control the total amount of RAGE, 1/10 of the supernatant was analyzed by Western blotting. Densitometry was carried out within the linear range of the films.

Antibody-mediated internalization assay: receptor clustering-mediated internalization

Antibody-mediated internalization is a technique that has been extensively applied to investigate the endocytic fate of various receptors and membrane-associated proteins (Tiruppathi et al., 1997; Piazza et al., 2005; Millan et al., 2006; Tampellini et al., 2007).

Schwann cells were growth on glass coverslips coated with 1 $mg\,ml^{-1}$ poly-L-lysine and starved in SCDM for 24 h. Rabbit anti-RAGE antibody (1 $\mu g\,ml^{-1}$) (H-300, Santa Cruz Biotechnology, Inc., Santa Cruz, CA) was added to the SC for 30 min at 4°C in incubation medium (DMEM, 10 mM Hepes pH 7.5, 0.2% BSA). The specificity of this antibody has been previously verified and it has been employed to detect RAGE subcellular localization in vesicles by co-localization experiments and immunofluorescence analysis (Hermani et al., 2006). For internalization studies, cells were fixed either immediately after incubation at 4°C (0 min, indicating surface labeled RAGE) or following incubation at 37°C for various times to induce the internalization of RAGE-antibody complex (Tampellini et al., 2007). Indeed, the incubation of the cells at 4°C completely block the endocytic machinery and RAGE ligands are not internalized (Schmidt et al., 1993). Briefly, cells were washed twice with ice cold PBS containing 1.8 mM Ca^{2+} and 0.5 mM Mg^{2+} (PBS/CM) to eliminate the unbound antibody, incubated at 37°C in SCDM for different times, then washed twice with ice cold PBS/CM and fixed for 20 min with 4% paraformaldehyde (PFA) in PBS. To verify that in the absence of incubation at 37°C the antibody labels only surface RAGE, while it is internalized together with RAGE following incubation at 37°C, we performed a confocal Z stack analysis (Tampellini et al., 2007). Control cells (0 min) and cells incubated for 5 min at 37°C were permeabilized (see below) and the localization of the RAGE-antibody complex and phosphorylated cav1 were investigated by immunofluorescence and confocal analysis performing Z-stack sections from the bottom of the cells (adhesion of the cells to the cover slips) to the top of the cells. Optical sections were acquired at 0.7 μm thickness (supplemental Figs. S1 and S2). For confocal analysis, cells were treated for 5 min with PBS/CM containing 0.15% TX-100, blocked with PBS/CM, 0.05% TX-100 and 1% bovine albumin for 30 min. Cells were incubated at room temperature for 1 h with biotin-conjugated anti rabbit IgG (1:400) (Sigma–Aldrich, catalog number: B7389) and the appropriate antibody for the double staining: mouse anti-phospho-cav-1 (1:25) (Tyr14 BD; BD Transduction, BD Biosciences, catalog number 611338), mouse anti-Rab11 (1:200) (BD Biosciences. Clone 47, catalog number 610656), mouse anti-S100 (1:100) (Chemicon, Millipore, Bilerica, MA, catalog number MAB079-1). Fluorescein isothiocyanate (FITC)-conjugated streptavidin and Texas-Red-conjugated anti-mouse IgG were used for staining (Molecular Probes, Invitrogen, Carlsbad, CA).

Lysosomes were detected by incubating the cells with LysoTracker Red (1:10,000) (Molecular Probes, Invitrogen, catalog number L-7528) 30 min before antibody-mediated RAGE internalization. Specimens were mounted in ProLong gold mounting medium containing DAPI (Invitrogen).

Analysis of immunofluorescence was performed with an Olympus FluoView 500 laser scanning confocal microscope. Samples were visualized with an Olympus IX-71 inverted microscope using a 60× oil-immersion lens, magnified two times with FluoView version 5.0 software and scanned sequentially to maximize signal separation. DAPI, AlexaFluor 488 and AlexaFluor 594 fluorescence were excited with a 405 nm blue laser diode, 488 nm argon blue and 543 nm helium neon laser, respectively. Emissions were separated with 430–460 nm, 505–525 nm, and 610+ nm barrier filters.

Immunofluorescence analysis after stimulation with bovine brain S100

To obtain synchronous stimulation of surface RAGE, cells were stimulated with bovine brain S100 at 4°C for 30 min. Unbound S100 were washed with ice-cold PBS/CM, and cells were incubated at 37°C for different times. Cells were fixed in 4% PFA in PBS/CM for 20 min. They were then washed twice with PBS/CM and once with NH_4Cl 5 mM in PBS/CM to quench the excess PFA. Cells were permeabilized 5 min with TX-100 0.15% in PBS/CM and blocked for 30 min in PBS/CM containing 0.05% TX-100 and 1% BSA. Cells were incubated for 1 h at room temperature with the primary antibody: rabbit anti-dynamin (H-300) (1:100) (SantaCruz Biotechnology, Inc., catalog number sc-11362); mouse anti-phospho cav1 (1:25) (Tyr14 BD Transduction, BD Biosciences, catalog number 611338). They were then washed three times for 10 min with PBS/CM and incubated for 1 h at room temperature with the fluorochrome-labeled secondary antibody (Molecular Probes, Invitrogen). The morphology of SC was examined under the same conditions. Immunofluorescence was analyzed with an Olympus FluoView 500 laser scanning confocal microscope as described above.

Treatment with high glucose

To investigate the effect of high glucose on SC morphology, cells were growth in 50 mM glucose for 24 h, serum-starved in 50 mM glucose for an additional 24 h before stimulation.

Immunoprecipitation and immunoblot analysis

Cells were washed twice with ice-cold PBS/CM and lysed as described elsewhere (Jori et al., 2003). Samples were immunoprecipitated with the following antibodies: rabbit anti-cav-1 1:100 (N-20, Santa Cruz Biotechnology, Inc., catalog number sc-894), rabbit polyclonal anti-RAGE 1:100 (H-300, Santa Cruz Biotechnology, Inc., catalog number sc-5563), mouse anti-c-src 1:100 (Upstate/Millipore, catalog number 05-184).

Western blot analysis was carried out with the following antibodies: mouse anti-phospho-cav-1 1:500 (Tyr14, BD Transduction, catalog number 611338), rabbit anti-cav-1 1:1,000 (BD Transduction, catalog number 610406), mouse anti-RAGE 1:500 (RD Systems, catalog number MAB1179), mouse anti-S100B 1:1,000 (Chemicon, catalog number MAB079-1), HRP-conjugated streptavidin 1:5,000 (Pierce Chemical Co., catalog number N200). Rabbit anti-phospho Fak (Santa Cruz Biotechnology, Inc., catalog number sc-16563-R), anti-Fak (BD Transduction, catalog number 610088). Rabbit anti phospho-src (1:1,000) (Calbiochem, EMD Biosciences, catalog number 569373). Mouse anti-c-src 1:1,000 (Santa Cruz Biotechnology, Inc., catalog number sc-5266).

To inhibit RAGE-S100 interaction, cells were incubated with a blocking antibody against rat RAGE (25 μg/ml) (RD System Minneapolis, MN, catalog number: AF1179) for 30 min at 4°C. Cells were then treated with bovine-brain S100 20 μg/ml at 37°C. Anti-RAGE blocking antibodies from RD System were previously used to inhibit the interaction of RAGE with the ligand (Hermani et al., 2006; Sakaguchi et al., 2008). The blocking antibody is not suitable for immunofluorescence analysis as indicated by the manufacturer instruction and a previous report (Hermani et al., 2006).

Results

RAGE is internalized and recycles at the plasma membrane after stimulation with S100

To correlate the endocytic trafficking of RAGE with its physiological function in SC, we analyzed the endocytic trafficking of endogenous RAGE in primary cultures of SC. To determine whether RAGE is degraded or recycles to the plasma membrane after S100 stimulation, we used an endocytosis assay based on the use of a cleavable biotin analog (Perrone et al., 2005). After biotinylation, SC were treated with bovine brain S100 (20 μg/ml), a well-defined RAGE activator (Hofmann et al., 1999; Vincent et al., 2007), for 0, 5, 20, and 60 min in duplicate. The sample treated with glutathione shows whether the receptor is endocytosed because internalized receptor is not accessible to glutathione. The sample not treated with glutathione represents the total amount of biotinylated receptor during stimulation. After stimulation with S100 for 5 and 20 min, biotinylated RAGE was in an endocytic compartment (Fig. 1A, lanes 3–6). After 60 min of stimulation, biotinylated RAGE was again available for glutathione cleavage, whereas the total amount of biotinylated RAGE was reduced by only 20% (Fig. 1A, lanes 7, 8). Thus, about 80% of RAGE recycles at the plasma membrane after 60 min of S100 stimulation. Biotinylation does not affect RAGE subcellular localization or signaling either under steady-state conditions or upon stimulation with S100 (data not shown).

We next analyzed the half-life of RAGE with and without S100 stimulation. Schwann cells were treated with cycloheximide (CHX, 50 μg/ml) and incubated with and without S100. In the absence of S100, RAGE decreased after 3 h of incubation with CHX and was greatly reduced after 16 h (Fig. 1B, lanes 5 and 6). On the contrary, RAGE was unvaried up to 16 h of incubation with CHX in the presence of S100 (Fig. 1B, lanes 1–4).

We monitored the endocytic trafficking of RAGE using antibody ligation-induced internalization (Tiruppathi et al., 1997; Piazza et al., 2005; Millan et al., 2006; Tampellini et al., 2007). The anti-RAGE antibody used in this assay induces both the internalization (Fig. 1C) and signaling of RAGE (Fig. 2A, lane 4). Cells were incubated 30 min at 4°C with anti-RAGE antibody, washed and incubated at 37°C for 5 min. Internalized RAGE was targeted to a perinuclear compartment and co-localized with Rab11 after 5 min of incubation at 37°C (Fig. 1C). After stimulation with S100 both internalized RAGE and Rab11 were localized in the perinuclear compartment, whereas in the absence of S100, RAGE was distributed over the whole cell surface (Fig. 1C). Internalized RAGE did not co-localize with lysosomes (data not shown). These data demonstrate that RAGE is targeted to the recycling pathway after interaction with the ligand.

Src-mediated phosphorylation of cav-1 is required for RAGE recycling at the plasma membrane

Phosphorylated cav-1 is involved in endocytic trafficking (Tiruppathi et al., 1997; del Pozo et al., 2005). Since RAGE activation results in src-mediated phosphorylation of cav-1 in endothelial smooth muscle cells (Reddy et al., 2006), we sought to examine whether stimulation of RAGE induces src-mediated cav1 phosphorylation in SC. Src was activated after 5 min of treatment with bovine brain S100 (Fig. 2A, lane 2). Src activation was RAGE-dependent. Indeed, a RAGE-blocking antibody strongly reduced S100-induced src activation

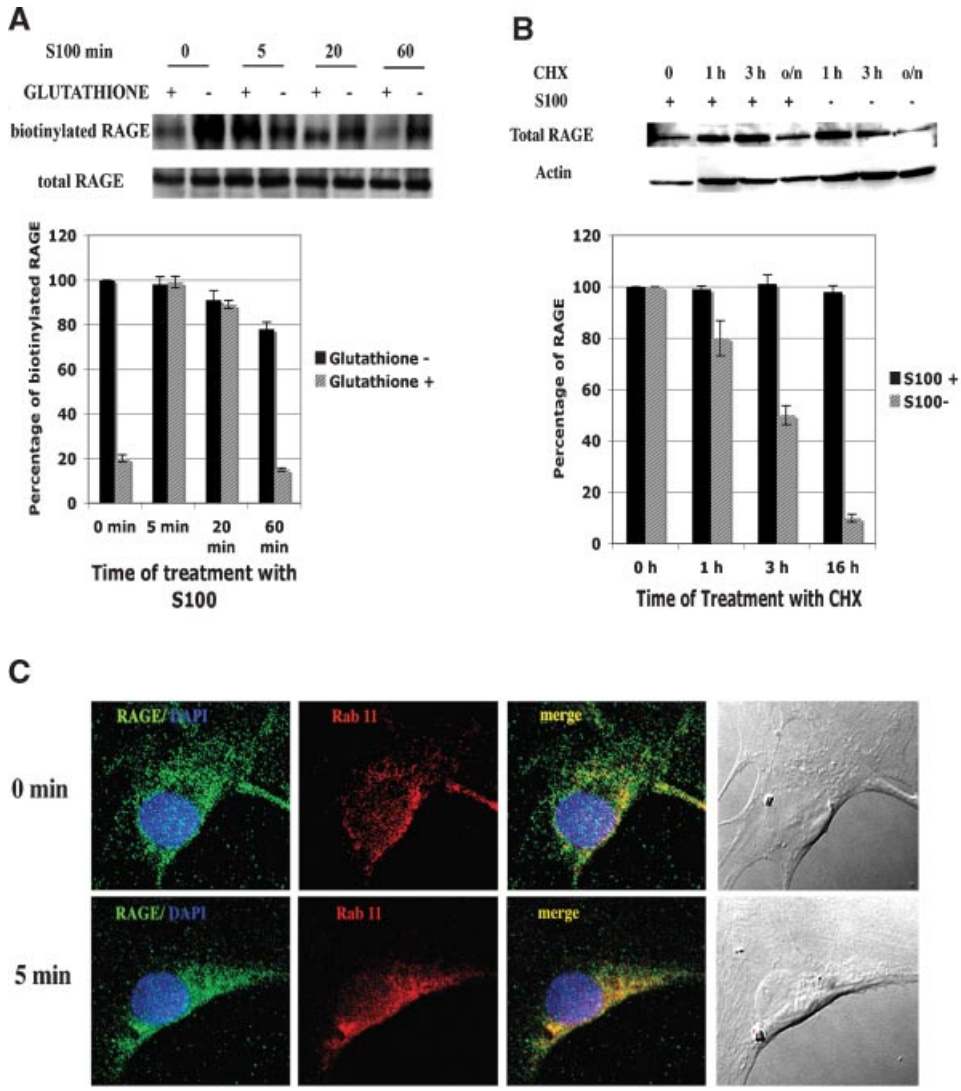

Fig. 1. RAGE is targeted to the recycling pathway upon stimulation. A: SC were surface biotinylated with NHS-SS-biotin and then incubated at 37°C with bovine brain S100 (20 μg ml^{-1}). Biotinylated and total RAGE were detected by Western blotting. Quantification of three independent experiments is shown at the bottom of the figure. B: SC were treated with cycloheximide (15 μg/ml) and S100 (20 μg ml^{-1}) as indicated. RAGE was detected by Western blotting. Quantification of three independent experiments is shown at the bottom of the figure. C: RAGE internalization (green) was induced by antibody-mediated internalization. The localization of internalized RAGE (green) and Rab11 (red) was evaluated by immunofluorescence and confocal analysis. The scale bar indicates 10 mm. These experiments are representative of at least three independent experiments. [Color figure can be viewed in the online issue, which is available at www.interscience.wiley.com.]

(Fig. 2A, lane 3). On the contrary, unspecific IgG did not inhibit S100-mediated src phosphorylation (Fig. 2A, lane 5). RAGE triggering by an antibody against the extracellular domain of RAGE also induced src phosphorylation, which confirms that src-induction is RAGE-dependent (Fig. 2A, lane 4).

We next investigated whether RAGE activation induces cav-1 phosphorylation. Cav-1 phosphorylation increased fourfold after 5 min of stimulation with bovine brain S100 (Fig. 2B, compare lanes 1 and 2). Cav1 phosphorylation was src-dependent. Indeed, the src-specific inhibitor PP1 (Khan et al., 2006) totally abolished S100-mediated cav1 phosphorylation (Fig. 2B, lane 3). The antibody against the extracellular domain of RAGE also increased cav1 phosphorylation sixfold thereby demonstrating that RAGE triggering induces cav1 phosphorylation (Fig. 2B, lane 4). To assess whether phosphorylated cav1 is involved in RAGE endocytic trafficking, we investigated the localization of phosphorylated cav1 and RAGE by antibody ligation-induced internalization. RAGE did not co-localize with phospho-cav-1 in the absence of activation at 37°C (Fig. 2C), whereas internalized RAGE co-localized with phospho-cav-1 in a perinuclear compartment after 5 and 20 min of incubation at 37°C (Fig. 2C). Phosphorylated cav1 was relocated in the perinuclear compartment after RAGE activation, whereas it was localized exclusively at the plasma membrane in the absence of RAGE triggering (Fig. 2C). RAGE and phosphorylated cav1 co-localized in a perinuclear region also after stimulation with bovine brain S100 (data not shown). Confocal Z stack images demonstrate that endocytosis of surface RAGE does not occur at 4°C. Indeed, the uptake of anti-RAGE antibody is blocked when cells are fixed at 0 min. Following permeabilization of the cells, the staining of RAGE-antibody complex is evident only in

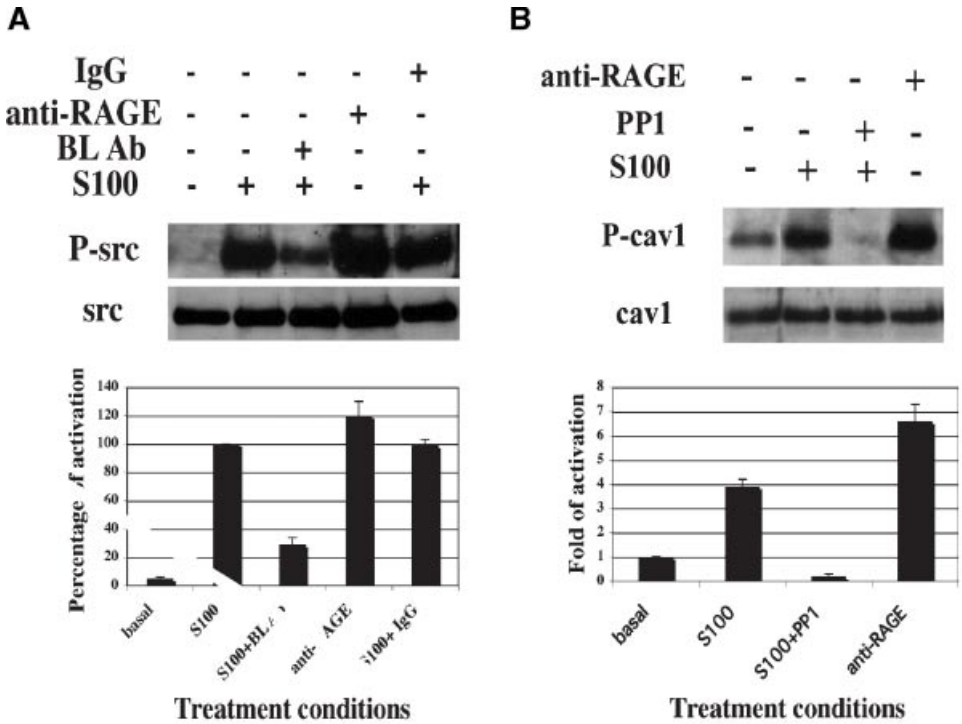

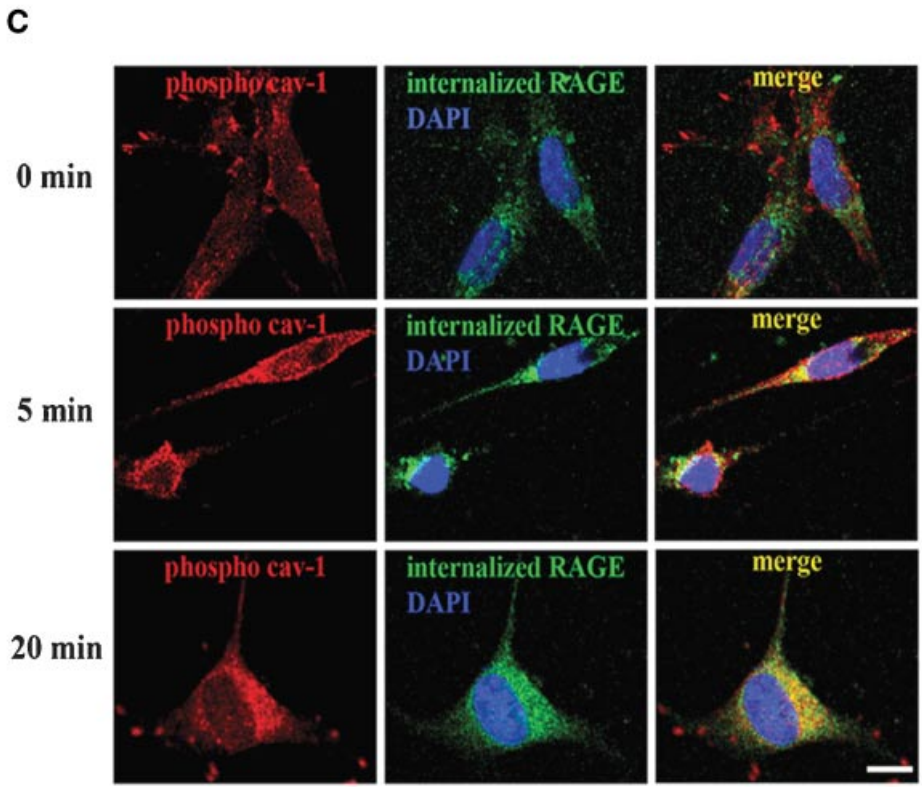

Fig. 2. Phosphorylated cav-1 targets RAGE to the recycling pathways. A: SC were stimulated with S100 (20 μg ml^{-1}) for the indicated time with and without an anti-RAGE blocking antibody (BL Ab), anti-RAGE activating antibody, or unspecific IgG. Protein extracts were immunoprecipitated with a mouse anti-src antibody. Phosphorylated src and src were detected by Western blotting. Quantification of three independent experiments is shown at the bottom of the figure. B: SC were stimulated as in (A). Protein extracts were immunoprecipitated with an anti-cav1 antibody. Phosphorylated cav1 and cav1 were detected by Western blotting. Quantification of three independent experiments is shown at the bottom of the figure. C: Internalization of RAGE (green) was induced by antibody-mediated internalization and incubation at 37°C for the indicated times. Internalized RAGE (green) and phosphorylated cav-1 (red) were detected by immunofluorescence and confocal microscopy. The scale bar indicates 10 μm. Bl Ab = anti-Rage blocking antibody. [Color figure can be viewed in the online issue, which is available at www.interscience.wiley.com.]

sections corresponding to the cell surface and does not co-localize with phosphorylated cav1 in any of the Z-scan sections (supplemental Fig. S1). Incubation at 37°C for 5 min leads to relocation of RAGE-antibody complex to the intracellular compartment, as demonstrated by confocal Z scan images following permeabilization of the cells. There is no evident staining of RAGE-antibody complex at the plasma membrane (top sections), while it is localized in an intracellular compartment where it co-localizes with phosphorylated cav-1 (supplemental Fig. S2). In the absence of cell permeabilization, the staining of RAGE-antibody complex is evident at 0 min, while it is strongly reduced following 5 min of incubation at 37°C (data not shown). Since after incubation at 37°C the staining of RAGE-antibody complex is evident only following permeabilization of the cells, we further demonstrate that the uptake of anti-RAGE antibody is blocked at 4°C and that RAGE-antibody complex is internalized following incubation at 37°C.

We next investigated whether phosphorylation of cav-1 plays a functional role in RAGE endocytic trafficking. To this aim, cells were pre-treated with 5 μM PP1 for 45 min to inhibit src-mediated cav-1 phosphorylation (Khan et al., 2006). This experiment confirmed that RAGE recycles at the plasma membrane after 60 min of stimulation with bovine brain S100 (Fig. 3A, lanes 1–4). Biotinylated RAGE was greatly reduced in the presence of PP1 and glutathione cleavage (about 85% compared with control time 0 min without glutathione cleavage). It was also greatly reduced in the presence of PP1 and in the absence of glutathione cleavage (about 80% compared with control time 0 min), suggesting that src-inhibition induces RAGE degradation after S100 stimulation. We used biotinylation-based degradation assays (Jullien et al., 2002; Tanowitz and Von Zastrow, 2002; Chen et al., 2005; Tampellini et al., 2007) to determine whether inhibition of src activation changes the trafficking fate of RAGE. Cells were biotinylated and stimulated with bovine brain S100 at 37°C for different times in the presence and absence of PP1. Without PP1, biotinylated RAGE was reduced (by about 30%) after 3 h of S100 stimulation. On the contrary, in the presence of PP1, biotinylated RAGE was reduced by about 72% after 1 h of S100 stimulation (Fig. 3B). Using antibody-cross linking-mediated internalization, we found that RAGE is targeted to lysosomes after 30 min of S100 stimulation in the presence of PP1 (Fig. 3C).

We then examined the localization of internalized RAGE and Rab11 after 5 min of antibody-cross linking-mediated internalization both with and without PP1-induced src inhibition. We observed a reduction of RAGE-Rab11 co-localization in the presence of PP1 compared to the control stimulated in the absence of PP1 (Fig. 3D).

Accordingly, the endocytosis assay showed that about 20% of biotinylated RAGE recycles at the plasma membrane (Fig. 3A). These data demonstrate that inhibition of src changes the trafficking fate of internalized RAGE. Indeed, in the presence of PP1, about 80% of RAGE was targeted for degradation, whereas only 20% was still targeted to the recycling pathway.

RAGE-induced secretion of S100B requires src activation

Although RAGE induces S100B relocation in vesicles in endothelial cells (Hsieh et al., 2004), the trafficking pathway responsible for S100B translocation in vesicles is unknown. Since SC express endogenous S100B, we investigated whether RAGE triggering affects S100B exocytic trafficking using the antibody-mediated internalization assay. As shown in Figure 4A, RAGE and S100B did not co-localize in the absence of induction of endocytosis by incubation of the cells at 37°C (time 0-min in Fig. 4A). Internalized RAGE co-localized with S100B in vesicle-like structures in the perinuclear region upon 5 min of internalization at 37°C. RAGE and S100B still co-localized after 20 and 60 min of internalization and were distributed throughout the cytoplasm. The relocalization of S100B in vesicles was mediated by RAGE triggering. Indeed, in cells treated with an unspecific IgG and incubated at 37°C for 5 min, no vesicles were S100B-positive, whereas S100B appeared in the cytoplasm.

PP1 inhibited RAGE co-localization with endogenous S100B (Fig. 4B). S100B and internalized RAGE were localized in a perinuclear compartment after 60 min of RAGE triggering in the presence of PP1; however, the co-localization was very low and S100B and RAGE staining was weak (Fig. 4B). S100B relocation in vesicles is Ca^{2+}-dependent in astrocytoma cells (Mbele et al., 2002). RAGE triggering in the presence of 10 mM EGTA inhibited S100B co-localization with RAGE (data not shown), which is in agreement with a previous finding (Davey et al., 2001).

We also investigated the RAGE-S100B association in co-immunoprecipitation experiments using an anti-RAGE antibody. Stimulation with exogenous bovine brain S100 greatly increased the amount of S100B in the immunocomplex (about sevenfold induction compared with unstimulated cells) (Fig. 4C, lane 2). Although we do not know whether RAGE co-immunoprecipitates with endogenous or extra-cellular S100B or both, this observation could suggest that RAGE does not dissociate from extracellular S100. In agreement, RAGE is responsible for the transcytosis of the β-amyloid peptide from the apical to the basolateral surface in endothelial cells, further demonstrating that RAGE does not dissociate from the ligand during its endocytic trafficking (Mackic et al., 1998).

Astrocytes secrete S100B consequent to metabolic stress (Gerlach et al., 2006). Since SC express endogenous S100B, we sought to determine whether RAGE activation induces secretion of endogenous S100B. To this aim, we stimulated RAGE using antibody-mediated internalization to identify endogenous S100B in the media, and used Western blotting to evaluate S100B secretion after tri-fluoro acetic acid (TCA) precipitation of the culture medium (Pachydaki et al., 2006). To quantify the cell number stimulated in the different conditions, we measured the amount of actin by Western blot (Fig. 4D, bottom). S100B was not detectable in the media in the absence of stimulation or after 20 min of RAGE triggering, whereas it was secreted after 60 and 120 min of RAGE triggering (Fig. 4D, lanes 1–4). S100B secretion was src-dependent and was completely abolished in the presence of PP1 (Fig. 4D, lane 5). Treatment of SC with PP1 in the presence of an unrelated antibody instead of anti-RAGE antibody did not induce S100B secretion (Fig. 4D, lane 6), which confirms that RAGE triggering is required for S100B secretion.

High glucose inhibits RAGE-induced src activation

RAGE plays a key role in the development of diabetes (Bierhaus et al., 2005). However, the effect of a HG concentration on RAGE function in SC is unknown. In an attempt to shed light on this issue, we first analyzed the effect of HG on RAGE-mediated src activation after S100 stimulation. In culture medium with a physiological glucose concentration (5.5 mM = LG), src was activated in response to S100 stimulation, whereas 50 mM glucose (HG) inhibited RAGE-mediated src activation to the same extent as PP1 (Fig. 5A lanes 1–4, and 6). High glucose did not affect src phosphorylation in the absence of S100 stimulation (Fig. 5A, lane 5), neither did it affect cell viability (data not shown). We next investigated Fak phosphorylation after RAGE triggering. Fak activation was delayed despite src phosphorylation; it occurred after 10 min of RAGE triggering and persisted up to 15 min of stimulation (Fig. 5B, lanes 1–4). Inhibition of src activation with PP1 completely abolished Fak phosphorylation (Fig. 5B, lane 5). High glucose also inhibited RAGE-mediated Fak activation (Fig. 5B, lane 6). It did not affect

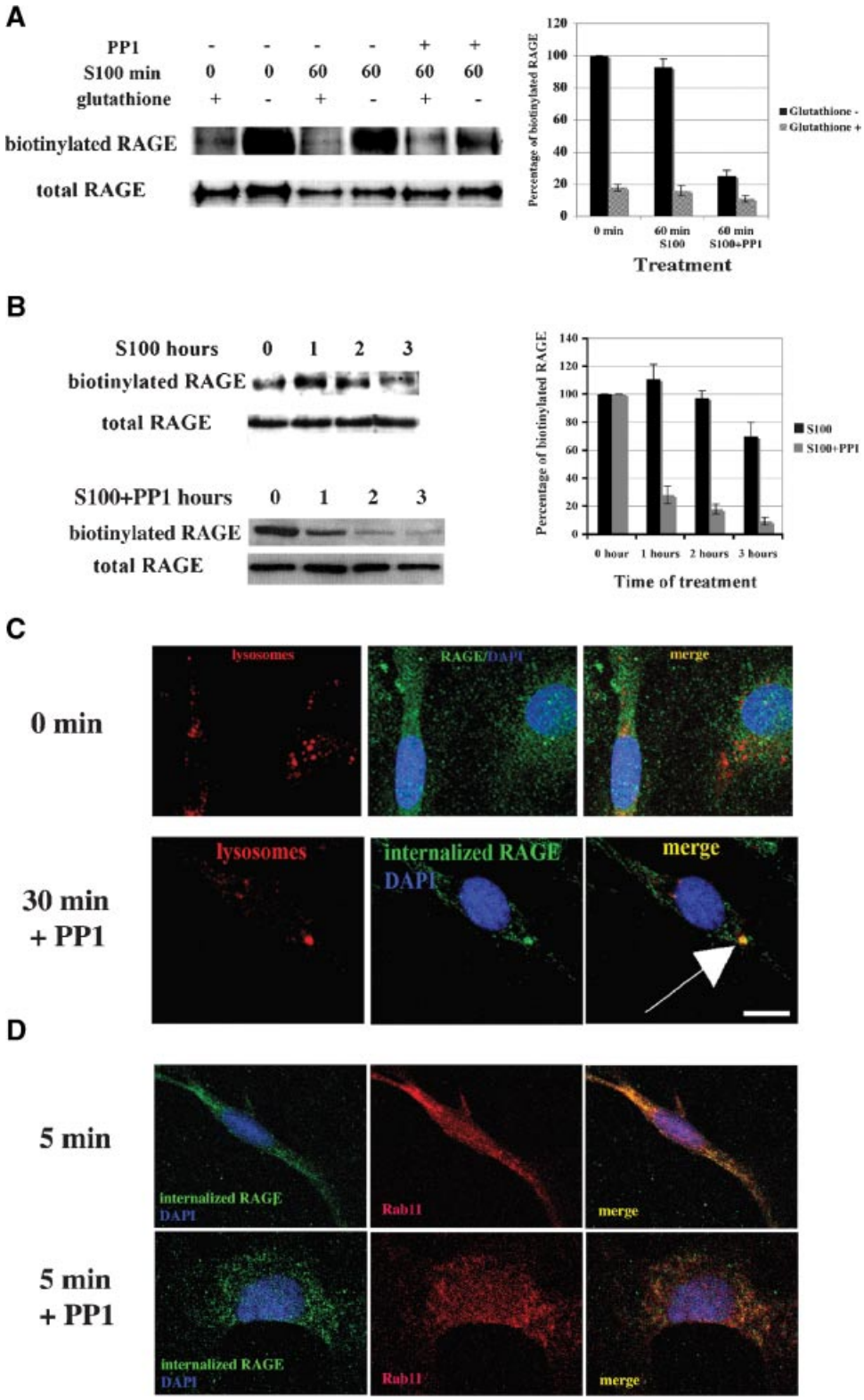

Fig. 3. src activation is necessary for RAGE recycling at the plasma membrane. A: SC were incubated with src-specific inhibitor PP1. Control and PP1-treated cells were surface biotinylated with NHS-SS-biotin and incubated at 37°C with S100 (20 μg ml^{-1}) for the indicated times. Biotinylated RAGE was detected by Western blotting after pull-down with avidin beads (top). Total RAGE was analyzed by Western blotting. Quantification of three independent experiments is shown at the right of the figure. B: Cells were surface biotinylated with NHS-LC-biotin and incubated at 37°C with S100 (20 μg ml^{-1}) for the indicated times. Biotinylated RAGE was detected by Western blotting after pull-down with avidin beads (top). Total RAGE was evaluated by Western blotting. Quantification of three independent experiments is shown at the right of the figure. C: Internalization of RAGE (green) was induced by antibody-mediated internalization. Cells were incubated at 37°C for 30 min with PP1. Control cells were fixed immediately after antibody-mediated RAGE internalization. Lysosomes were detected by incubating the cells with Lysotraker (red). The scale bar indicates 10 mm. D: Internalization of RAGE was carried out as in (C) both with and without PP1. The localization of internalized RAGE (green) and Rab11 (red) was evaluated with immunofluorescence and confocal microscopy. These experiments are representative of at least three independent experiments. [Color figure can be viewed in the online issue, which is available at www.interscience.wiley.com.]

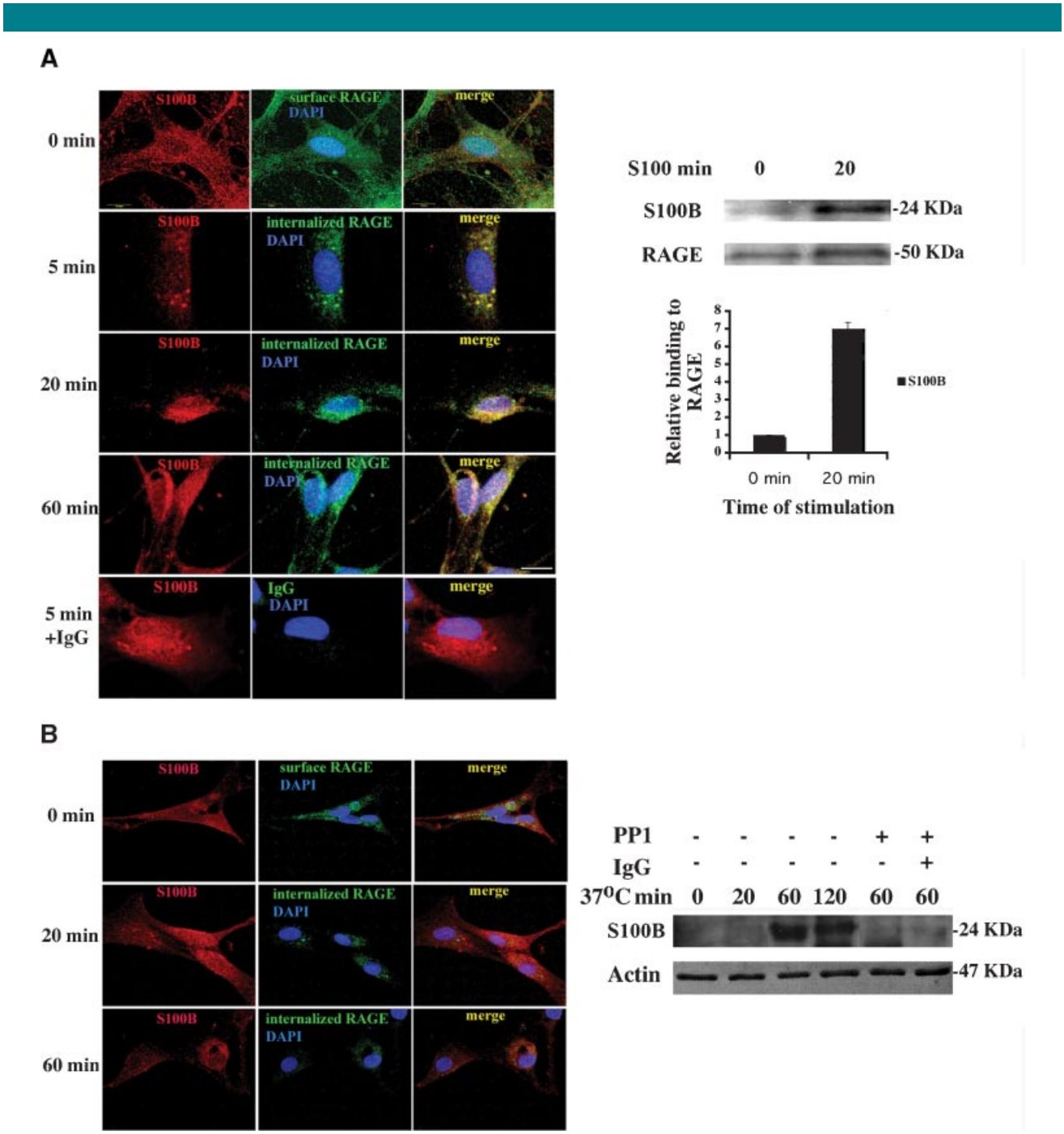

Fig. 4. Internalized RAGE co-localizes with endogenous S100B. A,B: Internalization of RAGE was induced by antibody-mediated internalization. The localization of internalized RAGE (green) and S100B (red) was evaluated with immunofluorescence and confocal microscopy. As control, cells were treated with unspecific IgG instead of with anti-RAGE antibody and incubated at 37°C for 5 min (bottom). B: RAGE internalization was carried out as in (A). Cells were treated with PP1. The localization of internalized RAGE (green) and S100B (red) was evaluated with immunofluorescence and confocal microscopy. The scale bar indicates 10 mm. C: SC were stimulated with S100 for 20 min. Protein extracts were immunoprecipitated using an anti-RAGE antibody. S100B and RAGE were detected by Western blotting. Quantification of three independent experiments is shown at the bottom of the figure. D: Internalization of RAGE was induced by antibody-mediated internalization both in the presence and absence of PP1. As control, cells were incubated with unspecific IgG instead of anti-RAGE antibody and incubated at 37°C in the presence of PP1. Cells were incubated with fresh medium after antibody-mediated RAGE internalization. The medium was collected at the indicated time and was precipitated using TCA. The presence of S100B was evaluated with Western blotting. The amount of actin was evaluated with Western blotting as a control of the number of cells stimulated. These experiments are representative of at least three independent experiments. [Color figure can be viewed in the online issue, which is available at www.interscience.wiley.com.]

Fak phosphorylation in the absence of S100 stimulation (Fig. 5B, lane 7). This is in line with the finding that HG inhibits Fak activation in rat peritoneal mesothelial cells (Tamura et al., 2003).

Phosphatidylinositol 3-kinase (PI3K) activation induces Fak phosphorylation in SC (Cheng et al., 2000). We therefore investigated whether the PI3 kinase pathway is involved in RAGE-mediated Fak phosphorylation. The PI3K inhibitor

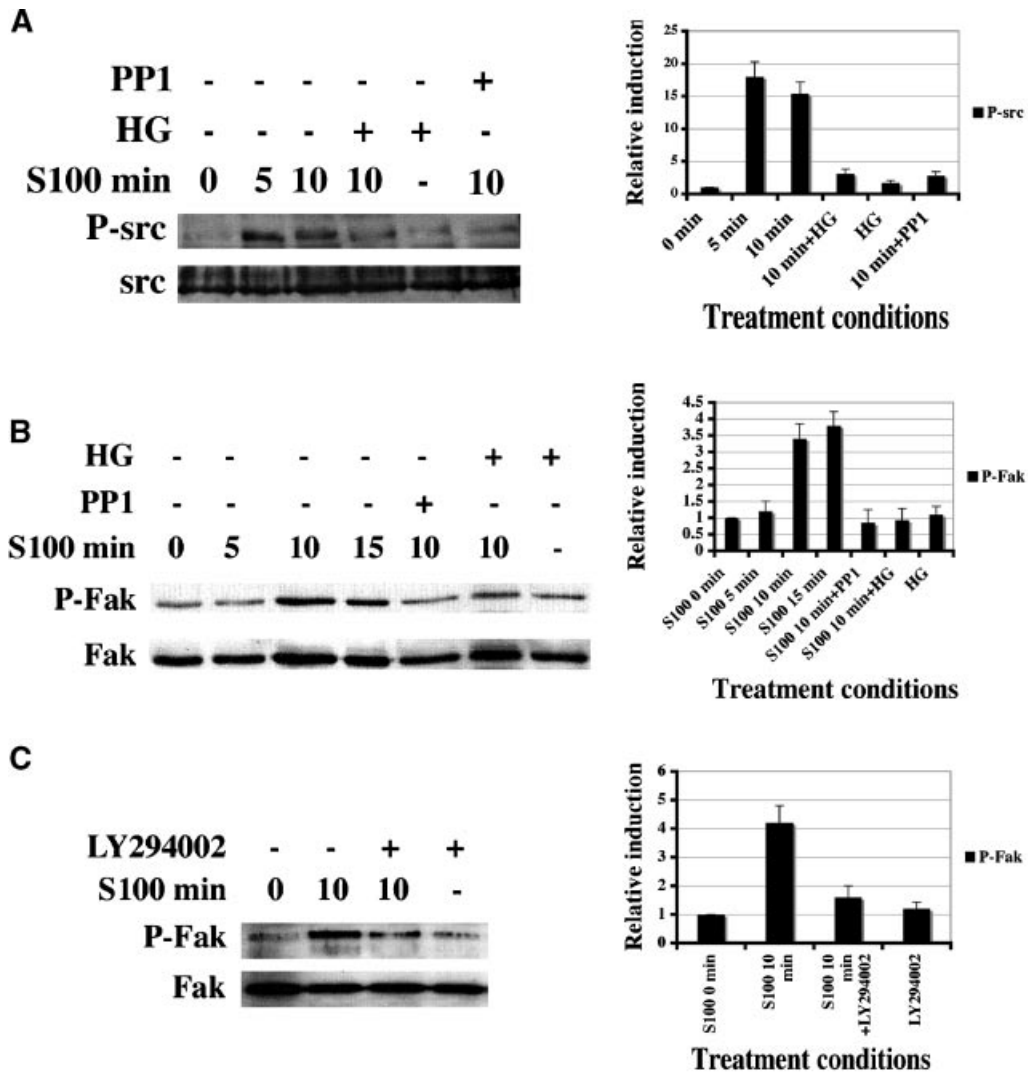

Fig. 5. HG inhibits S100-induced src and Fak phosphorylation. A: SC were stimulated with S100 (20 μg ml^{-1}) for the indicated time. PP1 was added as indicated. Cells were treated with HG (50 mM) for 48 h and during the stimulation where indicated. Protein extracts were immunoprecipitated with a mouse anti-src antibody. Phosphorylated src and src were detected by Western blotting. Quantification of three independent experiments is shown at the right of the figure. B: SC were stimulated as in A. Phosphorylated Fak and Fak were detected by western blotting. Quantification of three independent experiments is shown at the right of the figure. C: PI3K inhibitor LY294002 (10 μM) was added where indicated. Phospho Fak and Fak were detected by Western blotting. Quantification of three independent experiments is shown at the right of the figure. These experiments are representative of at least three independent experiments.

LY294002 completely blocked Fak phosphorylation in response to S100 stimulation (Fig. 5C, lane 3), whereas LY294002 did not affect Fak phosphorylation in the absence of stimulation with S100 (Fig. 5C, lane 4).

HG inhibits S100-induced phospho-cav1 and dyn2 co-localization and SC morphological changes

Since dynamins are involved in phosphorylated cav1-mediated endocytosis (del Pozo et al., 2005), we investigated the subcellular localization of dynamins after S100 stimulation. We incubated SC for 30 min with S100 at 4°C. Cells were then washed and incubated at 37°C for 30 sec and 5 min. Phosphorylated cav1 and dynamin did not co-localize in the absence of S100 stimulation (Fig. 6A). Phosphorylated cav1 was localized at the plasma membrane after 30 sec of stimulation, whereas dynamin showed filament-like structures in the cytoplasm (Fig. 6A). Interestingly, after 30 sec of stimulation, dynamin co-localized with phospho-cav1 only in one site at the plasma membrane, suggesting that remodeling of the adhesion occurs at this site (Fig. 6A). Phosphorylated cav1 co-localized with dynamin in a perinuclear compartment after 5 min of S100 stimulation (Fig. 6A). High glucose inhibited the perinuclear localization of phosphorylated cav1 after 5 min of S100 stimulation as well as its co-localization with dynamin (Fig. 6A). Compared with control cells, HG did not affect phosphorylated cav1 in the absence of stimulation with S100 (Fig. 6A).

We previously reported that morphological changes of neuroblastoma stem cells correlate with cellular differentiation (Jori et al., 2001). Given our present observation that RAGE induces Fak activation, and the finding that Fak activation is involved in SC motility (Cheng et al., 2000), we analyzed RAGE-mediated changes in SC shape. To this aim, we incubated

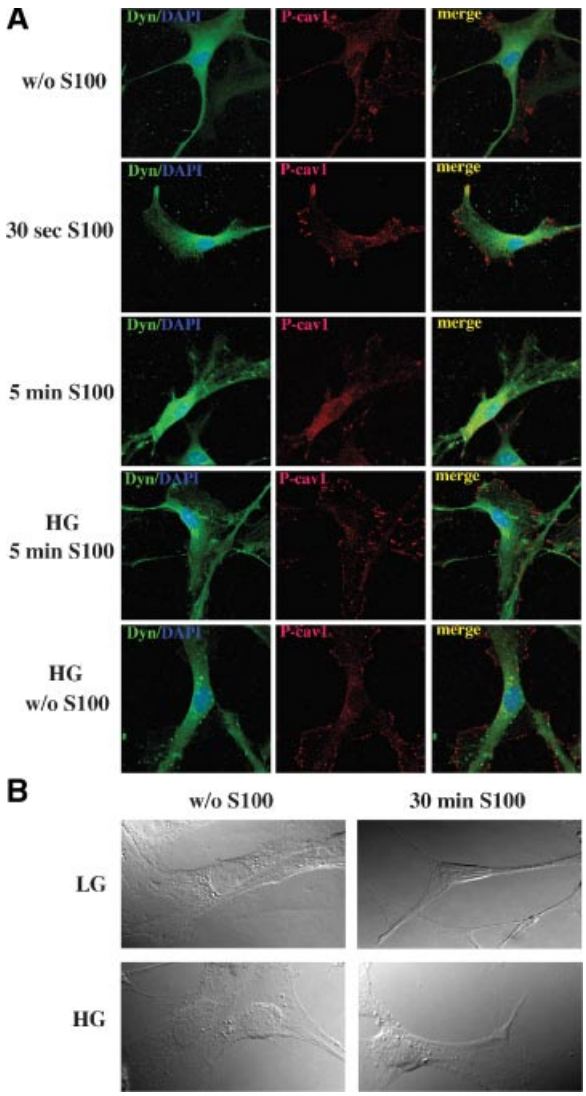

Fig. 6. HG inhibits S100-induced SC morphological changes. A: SC were stimulated with S100 (20 μg ml^{-1}) at 4°C for 30 min, washed and incubated at 37°C for the indicated time. HG (50 mM) was added as indicated. As a control, SC were incubated with HG in the absence of S100 (bottom). The intracellular localization of phosphorylated cav1 (red) and dyn2 (green) was analyzed by indirect immunofluorescence and confocal microscopy. B: SC were stimulated as in (A). Changes in cell shape were analyzed by phase contrast microscopy. These experiments are representative of at least three independent experiments. LG = low glucose; HG = high glucose. [Color figure can be viewed in the online issue, which is available at www.interscience.wiley.com.]

the cells for 30 min with bovine brain S100 at 4°C, and after removing unbound S100 by washing, we incubated the cells for 30 min at 37°C. Cells were fixed in 4% PFA and we examined their morphology by phase-contrast microscopy. Schwann cells acquired their characteristic bipolar shape after stimulation with S100, whereas they had a flattened fibroblast-like shape in the absence of S100 stimulation (Fig. 6B, top). High glucose partially inhibited the bipolar shape induced by S100. Indeed, in the presence of S100 and a HG concentration, SC started to elongate and to acquire the bipolar shape, although they retained a flat fibroblast-like morphology (Fig. 6B, bottom right). Without S100 stimulation and under HG conditions, SC assumed a fibroblast-like shape (Fig. 6B, bottom left).

Discussion

A previous study suggests that SC-mediated S100B secretion is required for peripheral nerve regeneration. Indeed, antibodies against S100B block peripheral nerve regeneration in vivo (Rong et al., 2004a). However, SC-mediated S100B secretion is still poorly investigated. SC are known to secrete a 12-kDa protein that induces neurite outgrowth in PC12 cells (Bampton and Taylor, 2005). In this report we demonstrate for the first time that SC secrete S100B. Also glioblastoma cells (Davey et al., 2001) and astrocytes (Gerlach et al., 2006) secrete S100B. However, the molecular mechanisms governing S100B secretion are still poorly understood. Several lines of evidence previously suggested that RAGE might be involved in the relocation in vesicles of various S100 family proteins. Indeed, stimulation of prostate cancer cells with the RAGE ligands S100A8/9 induced the co-location of RAGE with S100A8/9 in vesicles (Hermani et al., 2006). In endothelial cells, translocation of endogenous S100 proteins in vesicles is RAGE-dependent (Hsieh et al., 2004). The addition of exogenous S100A13 induced RAGE co-localization with endogenous S100A13, and pre-treatment with soluble RAGE inhibited S100A13 relocation in vesicles, which suggested that RAGE is required for S100A13 internalization and relocation of endogenous S100A13 in vesicles (Hsieh et al., 2004). However, neither RAGE internalization nor S100A13-RAGE co-localization was demonstrated. We provide the first demonstration that RAGE triggering induces RAGE internalization and the fusion of RAGE-containing endocytic vesicles with S100B-positive secretory vesicles (see model shown in Fig. 7A). Relocation of a specific S100 protein in vesicles was found to occur only when RAGE was stimulated with the same extracellular S100 protein, whereas it was inhibited by stimulation with a different member of S100 family (Hsieh et al., 2004). We show that triggering of RAGE with an anti-RAGE antibody induces S100B relocation in RAGE-positive endocytic vesicles. It is conceivable that different S100 proteins interact with specific proteins thereby activating specific trafficking pathways and inhibiting the translocation in vesicles of another member of the S100 protein family. Anti-RAGE antibody does not induce this effect. Here we demonstrate that anti-RAGE antibody induces RAGE internalization and signaling, as well as co-localization of internalized RAGE with endogenous S100B, which results in secretion of S100B. We also show that RAGE recycling correlates with S100B secretion. Indeed, as shown in Figure 7A, src orchestrates a hitherto unknown vesicular pathway that leads to RAGE recycling at the plasma membrane, fusion with S100B-containing vesicles, and S100B secretion. Inhibition of src activation leads to RAGE degradation and inhibits RAGE-S100B co-localization in vesicles as well as S100B secretion. In agreement with our model, it has been shown that RAGE triggers the internalization and the transcytosis of the Amyloid-β 1–40 peptide from the apical to the basolateral membrane in endothelial cells (Mackic et al., 1998). Indeed, Mackic et al. (1998) demonstrate that the degradation of the amyloid peptide is very low in endothelial cells, further supporting that internalized RAGE is not targeted to lysosomes. Eventual differences in the quantification of β-amyloid transcytosis in endothelial cells and RAGE recycling in SC can be due to the different methods used to investigate RAGE trafficking and/or the different cell type analyzed. In our experiments SC are not polarized, so we cannot evaluate whether RAGE is targeted to a transcytotic pathway. However, in agreement with our data in correlation with the Mackic et al. (1998) report, it has been demonstrated that src, cav-1 and dyn play a role in caveolae-mediated transendothelial transport (Shajahan et al., 2004a,b). Furthermore, RAGE co-fractionates with caveolae-rich membrane in endothelial cells (Lisanti et al., 1994) and we found that RAGE is lipid rafts associated and

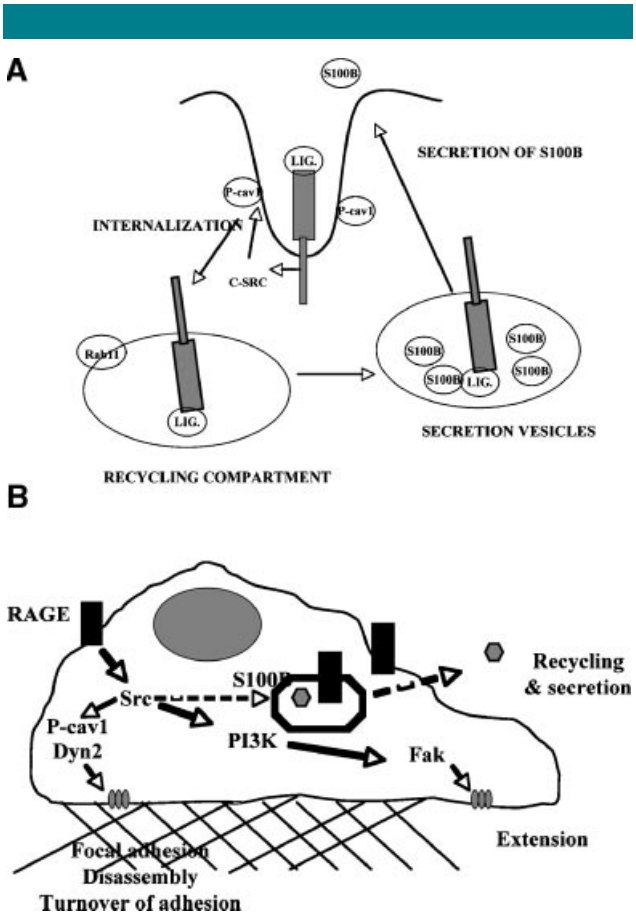

Fig. 7. Model for the autocrine stimulation of SC induced by RAGE triggering. A: Activation of RAGE induces src-mediated phosphorylation of cav-1 that targets RAGE to the recycling pathway in Rab11-positive vesicles. Internalized RAGE is targeted to vesicles containing endogenous S100B, which is secreted in response to RAGE activation. B: RAGE triggering induces src-mediated cav1 phosphorylation and re-location in the perinuclear compartment together with dyn2. Src orchestrates RAGE recycling, S100B secretion and morphological changes.

interact with cav-1 in SC (data not shown). Interestingly, the endocytic pathway here described for RAGE has been previously demonstrated for the gp60 receptor. Indeed, interaction of gp60 with either albumin or a gp60-specific antibody leads to src and cav-1 phosphorylation and induces gp60 internalization and targeting to the transcytotic pathway in endothelial cells (Tiruppathi et al., 1997). Further supporting our data compared with the Mackic et al. (1998) study, the function of Rab11 in transcytosis has also been demonstrated (Ducharme et al., 2007). Here we show that src-mediated phosphorylation of cav-1 is necessary for RAGE recycling at plasma membrane, while inhibition of src activation leads to RAGE targeting to lysosomes. The function of src-mediated phosphorylation of cav-1 in inhibiting receptor degradation and promoting a perinuclear targeting has been previously described for the EGF receptor (EGFR) (Khan et al., 2006). Indeed, it is well described that EGFR can follow two alternate pathways: be targeted to lysosomes for degradation or be transported to a perinuclear compartment via caveolae (Khan et al., 2006). Thus, the previous literature strongly support our observations summarized in Figure 7A. However, here we describe for the first time the role of cav-1 phosphorylation in the endocytic trafficking of RAGE and its function in promoting S100B secretion.

Here we show that RAGE triggering induces plasma membrane rearrangements. In agreement, S100B-mediated RAGE activation induces cell motility (Reddy et al., 2006). Receptor recycling and redistribution of membrane proteins play a role in cell motility (Jones et al., 2006). Indeed, we demonstrate that RAGE recycles through he Rab11 pathway. RAGE triggering induces phosphorylated cav1 translocation to the perinuclear compartment and co-localization with dynamin. Our data are in line with the finding that the dyn2 and Rab11 pathways contribute to cell migration (Jones et al., 2006).

Changes of cell shape require a coordinate disassembly and assembly of focal adhesions (Kruchten and McNiven, 2006). Interestingly, increment of cav1 phosphorylation inhibits Fak and causes disassembly of the actin cytoskeleton in (myo)fibroblasts (Swaney et al., 2006). In agreement, we demonstrate that phosphorylation of cav-1 is required for RAGE recycling, suggesting that RAGE-mediated src activation and subsequent cav-1 phosphorylation are responsible for S100-mediated SC morphological changes. Indeed, inhibition of src activation by high glucose treatment abolishes S100-mediated morphological changes of SC.

Our study shows that changes in SC shape correlate with S100B relocation in vesicles and S100B secretion. In agreement with this finding, relocation of S100B in vesicle-like structures correlates with membrane rearrangements in astrocytoma cells (Mbele et al., 2002). As shown in Figure 7B, we hypothesize a model whereby RAGE first induces an increase of cav1 phosphorylation thereby leading to disassembly of the focal adhesions. Next, perinuclear translocation of phosphorylated cav1 leads to rearrangement of focal adhesions. Indeed, endocytic trafficking of RAGE induces rearrangements of the plasma membrane. In the presence of S100, SC acquire the characteristic bipolar shape (Caddick et al., 2006), and show a differentiated-like phenotype with a reduction of the cytoplasm (Previtali et al., 2003). Changes in cell shape and cytoskeleton rearrangements are required to acquire the differentiate SC phenotype necessary to induce myelination (Previtali et al., 2003). SC myelinating phenotype is characterized by the expression of fibronectin (Akassoglou et al., 2002). We found that S100-mediated RAGE activation induces the mRNA expression of fibronectin (data not shown). Schwann cells, RAGE and S100 are required for peripheral nerve regeneration (Rong et al., 2004a,b; Dobrowsky et al., 2005). In agreement with our data, src is activated in SC after rat peripheral nerve injury (Zhao et al., 2003). We suggest that RAGE plays a key function in SC modifications that are important during regeneration of injured nerves.

We also demonstrate that HG inhibits RAGE-mediated src phosphorylation. Moreover, RAGE-mediated changes in SC shape do not occur under HG conditions. Given the involvement of src in cell motility (Cutrupi et al., 2000), this finding supports the concept that RAGE-mediated src activation plays a role in changes in SC shape. We demonstrate that inhibition of src activation induces RAGE degradation and blocks S100B secretion. In line with this observation, HG inhibits S100B secretion in astrocytes (Nardin et al., 2007). Further support for the physiological relevance of our data comes from the finding that regeneration of the injured sciatic nerve is delayed or fails in diabetes (Zochodne et al., 2007). Moreover, HG induces abnormal SC proliferation leading to a not differentiated phenotype that is characteristic of diabetic neuropathy (Almhanna et al., 2002). In agreement with these observations, we found that HG inhibits RAGE-induced fibronectin expression (data not shown).

In summary, we have identified a new vesicular pathway of RAGE recycling and S100B secretion, thereby providing insights into the role of RAGE in acquiring a pro-myelinating phenotype, while high glucose abolishes RAGE mediated effects on SC by inhibiting src activation.

Acknowledgments

This work utilized the Morphology and Image Analysis Core of the Michigan Diabetes Research and Training Center funded by NIH5P60 DK20572 from the National Institute of Diabetes & Digestive & Kidney Diseases. We thank C. Backus for assistance with SC. We also thank ME Bianchi, L Wrabetz, and L Franchi for the helpful discussion, and Jean Ann Gilder for text editing. LP would like to dedicate this work to the heart and soul of Silvana Geremia.

Literature Cited

Akassoglou K, Yu WM, Akpinar P, Strickland S. 2002. Fibrin inhibits peripheral nerve remyelination by regulating Schwann cell differentiation. Neuron 33:861–875.

Almhanna K, Wilkins PL, Bavis JR, Harwalkar S, Berti-Mattera LN. 2002. Hyperglycemia triggers abnormal signaling and proliferative responses in Schwann cells. Neurochem Res 27:1341–1347.

Bampton ET, Taylor JS. 2005. Effects of Schwann cell secreted factors on PC12 cell neuritogenesis and survival. J Neurobiol 63:29–48.

Berti C, Nodari A, Wrabetz L, Feltri ML. 2006. Role of integrins in peripheral nerves and hereditary neuropathies. Neuromolecular Med 8:191–204.

Bierhaus A, Humpert PM, Morcos M, Wendt T, Chavakis T, Arnold B, Stern DM, Nawroth PP. 2005. Understanding RAGE, the receptor for advanced glycation end products. J Mol Med 83:876–886.

Caddick J, Kingham PJ, Gardiner NJ, Wiberg M, Terenghi G. 2006. Phenotypic and functional characteristics of mesenchymal stem cells differentiated along a Schwann cell lineage. Glia 54:840–849.

Chavakis E, Hain A, Vinci M, Carmona G, Bianchi ME, Vajkoczy P, Zeiher AM, Chavakis T, Dimmeler S. 2007. High-mobility group box 1 activates integrin-dependent homing of endothelial progenitor cells. Circ Res 100:204–212.

Chen ZY, Ieraci A, Tanowitz M, Lee FS. 2005. A novel endocytic recycling signal distinguishes biological responses of Trk neurotrophin receptors. Mol Biol Cell 16:5761–5772.

Cheng HL, Steinway ML, Russell JW, Feldman EL. 2000. GTPases and phosphatidylinositol 3-kinase are critical for insulin-like growth factor-I-mediated Schwann cell motility. J Biol Chem 275:27197–27204.

Cutrupi S, Baldanzi G, Gramaglia D, Maffè A, Schaap D, Giraudo E, van Blitterswijk W, Bussolino F, Comoglio PM, Graziani A. 2000. Src-mediated activation of alpha-diacylglycerol kinase is required for hepatocyte growth factor-induced cell motility. EMBO J 19:4614–4622.

Davey GE, Murmann P, Heizmann CW. 2001. Intracellular Ca2+ and Zn2+ levels regulate the alternative cell density-dependent secretion of S100B in human glioblastoma cells. J Biol Chem 276:30819–30826.

Deane R, Du Yan S, Submamaryan RK, LaRue B, Jovanovic S, Hogg E, Welch D, Manness L, Lin C, Yu J, Zhu H, Ghiso J, Frangione B, Stern A, Schmidt AM, Armstrong D, Arnold B, Liliensiek B, Nawroth P, Hofman F, Kindy M, Stern D, Zlokovic B. 2003. RAGE mediates amyloid-beta peptide transport across the blood-brain barrier and accumulation in brain. Nat Med 9:907–913.

del Pozo MA, Balasubramanian N, Alderson NB, Kiosses WB, Grande-Garcia A, Anderson RG, Schwartz MA. 2005. Phospho-caveolin-1 mediates integrin-regulated membrane domain internalization. Nat Cell Biol 7:901–908.

Dobrowsky RT, Rouen S, Yu C. 2005. Altered neurotrophism in diabetic neuropathy: Spelunking the caves of peripheral nerve. J Pharmacol Exp Ther 313:485–491.

Ducharme NA, Williams JA, Oztan A, Apodaca G, Lapierre LA, Goldenring JR. 2007. Rab11-FIP2 regulates differentiable steps in transcytosis. Am J Physiol Cell Physiol 293:C1059–C1072.

Dumitriu IE, Bianchi ME, Bacci M, Manfredi AA, Rovere-Querini P. 2007. The secretion of HMGB1 is required for the migration of maturing dendritic cells. J Leukoc Biol 81:84–91.

Gerlach R, Demel G, Konig HG, Gross U, Prehn JH, Raabe A, Seifert V, Kogel D. 2006. Active secretion of S100B from astrocytes during metabolic stress. Neuroscience 141:1697–1701.

Hermani A, De Servi B, Medunjanin S, Tessier PA, Mayer D. 2006. S100A8 and S100A9 activate MAP kinase and NF-kappaB signaling pathways and trigger translocation of RAGE in human prostate cancer cells. Exp Cell Res 312:184–197.

Hofmann MA, Drury S, Fu C, Qu W, Taguchi A, Lu Y, Avila C, Kambham N, Bierhaus A, Nawroth P, Neurath MF, Slattery T, Beach D, McClary J, Nagashima M, Morser J, Stern D, Schmidt AM. 1999. RAGE mediates a novel proinflammatory axis: A central cell surface receptor for S100/calgranulin polypeptides. Cell 97:889–901.

Hsieh HL, Schafer BW, Weigle B, Heizmann CW. 2004. S100 protein translocation in response to extracellular S100 is mediated by receptor for advanced glycation endproducts in human endothelial cells. Biochem Biophys Res Commun 316:949–959.

Jones MC, Caswell PT, Norman JC. 2006. Endocytic recycling pathways: Emerging regulators of cell migration. Curr Opin Cell Biol 18:549–557.

Jori FP, Galderisi U, Piegari E, Peluso G, Cipollaro M, Cascino A, Giordano A, Melone MA. 2001. RB2/p130 ectopic gene expression in neuroblastoma stem cells: Evidence of cell-fate restriction and induction of differentiation. Biochem J 360:569–577.

Jori FP, Galderisi U, Piegari E, Cipollaro M, Cascino A, Peluso G, Cotrufo R, Giordano A, Melone MA. 2003. EGF-responsive rat neural stem cells: Molecular follow-up of neuron and astrocyte differentiation in vitro. J Cell Physiol 195:220–233.

Jullien J, Guili V, Reichardt LF, Rudkin BB. 2002. Molecular kinetics of nerve growth factor receptor trafficking and activation. J Biol Chem 277:38700–38708.

Kalichman MW, Powell HC, Mizisin AP. 1998. Reactive, degenerative, and proliferative Schwann cell responses in experimental galactose and human diabetic neuropathy. Acta Neuropathol (Berl) 95:47–56.

Khan EM, Heidinger JM, Levy M, Lisanti MP, Ravid T, Goldkorn T. 2006. Epidermal growth factor receptor exposed to oxidative stress undergoes Src- and caveolin-1-dependent perinuclear trafficking. J Biol Chem 281:14486–14493.

Kruchten AE, McNiven MA. 2006. Dynamin as a mover and pincher during cell migration and invasion. J Cell Sci 119:1683–1690.

Lisanti MP, Scherer PE, Vidugiriene J, Tang Z, Hermanowski-Vosatka A, Tu YH, Cook RF, Sargiacomo M. 1994. Characterization of caveolin-rich membrane domains isolated from an endothelial-rich source: Implications for human disease. J Biol Chem 126:111–126.

Mackic JB, Stins M, McComb JG, Calero M, Ghiso J, Kim KS, Yan SD, Stern D, Schmidt AM, Frangione B, Zlokovic BV. 1998. Human blood-brain barrier receptors for Alzheimer's amyloid-beta1-40. Asymmetrical binding, endocytosis, and transcytosis at the apical side of brain microvascular endothelial cell monolayer. J Clin Invest 102:734–743.

Mathon NF, Malcolm DS, Harrisingh MC, Cheng L, Lloyd AC. 2001. Lack of replicative senescence in normal rodent glia. Science 291:872–875.

Mbele GO, Deloulme JC, Gentil BJ, Delphin C, Ferro M, Garin J, Takahashi M, Baudier J. 2002. The zinc- and calcium-binding S100B interacts and co-localizes with IQGAP1 during dynamic rearrangement of cell membranes. J Biol Chem 277:49998–50007.

Mikol DD, Scherer SS, Duckett SJ, Hong HL, Feldman EL. 2002. Schwann cell caveolin-1 expression increases during myelination and decreases after axotomy. Glia 38:191–199.

Millan J, Hewlett L, Glyn M, Toomre D, Clark P, Ridley AJ. 2006. Lymphocyte transcellular migration occurs through recruitment of endothelial ICAM-1 to caveola- and F-actin-rich domains. Nat Cell Biol 8:113–123.

Nardin P, Tramontina F, Leite MC, Tramontina AC, Quincozes-Santos A, de Almeida LM, Battastini AM, Gottfried C, Gonçalves CA. 2007. S100B content and secretion decrease in astrocytes cultured in high-glucose medium. Neurochem Int 50:774–782.

Orlova VV, Choi EY, Xie C, Chavakis E, Bierhaus A, Ihanus E, Ballantyne CM, Gahmberg CG, Bianchi ME, Nawroth PP, Chavakis T. 2007. A novel pathway of HMGB1-mediated inflammatory cell recruitment that requires Mac-1-integrin. EMBO J 26:1129–1139.

Pachydaki SI, Tari SR, Lee SE, Ma W, Tseng JJ, Sosunov AA, Cataldergirmen G, Scarmeas N, Caspersen C, Chang S, Schiff WM, Schmidt AM, Barile GR. 2006. Upregulation of RAGE and its ligands in proliferative retinal disease. EXp Eye Res 82:807–815.

Perrone L, Paladino S, Mazzone M, Nitsch L, Gulisano M, Zurzolo C. 2005. Functional interaction between p75NTR and TrkA: The endocytic trafficking of p75NTR is driven by TrkA and regulates TrkA-mediated signalling. Biochem J 385:233–241.

Piazza T, Cha E, Bongarzone I, Canevari S, Bolognesi A, Polito L, Bargellesi A, Sassi F, Ferrini S, Fabbi M. 2005. Internalization and recycling of ALCAM/CD166 detected by a fully human single-chain recombinant antibody. J Cell Sci 118:1515–1525.

Previtali SC, Nodari A, Taveggia C, Pardini C, Dina G, Villa A, Wrabetz L, Quattrini A, Feltri ML. 2003. Expression of laminin receptors in schwann cell differentiation: Evidence for distinct roles. J Neurosci 23:5520–5530.

Reddy MA, Li S, Sahar S, Kim YS, Xu ZG, Lanting L, Natarajan R. 2006. Key role of Src kinase in S100B-induced activation of the receptor for advanced glycation end products in vascular smooth muscle cells. J Biol Chem 281:13685–13693.

Riuzzi F, Sorci G, Donato R. 2006. The amphoterin (HMGB1)/receptor for advanced glycation end products (RAGE) pair modulates myoblast proliferation, apoptosis, adhesiveness, migration, and invasiveness. Functional inactivation of RAGE in L6 myoblasts results in tumor formation in vivo. J Biol Chem 281:8242–8253.

Rong LL, Trojaborg W, Qu W, Kostov K, Yan SD, Gooch C, Szabolcs M, Hays AP, Schmidt AM. 2004a. Antagonism of RAGE suppresses peripheral nerve regeneration. FASEB J 18:1812–1817.

Rong LL, Yan SF, Wendt T, Hans D, Pachydaki S, Bucciarelli LG, Adebayo A, Qu W, Lu Y, Kostov K, Lalla E, Yan SD, Gooch C, Szabolcs M, Trojaborg W, Hays AP, Schmidt AM. 2004b. RAGE modulates peripheral nerve regeneration via recruitment of both inflammatory and axonal outgrowth pathways. FASEB J 18:1818–1825.

Sakaguchi M, Sonegawa H, Murata H, Kitazoe M, Futami J, Kataoka K, Yamada H, Huh NH. 2008. S100A11, a dual mediator for growth regulation of human keratinocytes. Mol Biol Cell 19:78–85.

Schindler T, Sicheri F, Pico A, Gazit A, Levitzki A, Kuriyan J. 1999. Crystal structure of Hck in complex with a Src family-selective tyrosine kinase inhibitor. Mol Cell 3:639–648.

Schmidt AM, Yan SD, Brett J, Mora R, Nowygrod R, Stern D. 1993. Regulation of human mononuclear phagocyte migration by cell surface-binding proteins for advanced glycation end products. J Clin Invest 91:2155–2168.

Shajahan AN, Timblin BK, Sandoval R, Tiruppathi C, Malik AB, Minshall RD. 2004a. Role of Src-induced dynamin-2 phosphorylation in caveolae-mediated endocytosis in endothelial cells. J Biol Chem 279:20392–20400.

Shajahan AN, Tiruppathi C, Smrcka AV, Malik AB, Minshall RD. 2004b. Gbetagamma activation of Src induces caveolae-mediated endocytosis in endothelial cells. J Biol Chem 279:48055–48062.

Swaney JS, Patel HH, Yokoyama U, Head BP, Roth DM, Insel PA. 2006. Focal adhesions in (myo)fibroblasts scaffold adenylyl cyclase with phosphorylated caveolin. J Biol Chem 281:17173–17179.

Tampellini D, Magrané J, Takahashi RH, Li F, Lin MT, Almeida CG, Gouras GK. 2007. Internalized antibodies to the Abeta domain of APP reduce neuronal Abeta and protect against synaptic alterations. J Biol Chem 282:18895–18906.

Tamura M, Osajima A, Nakayamada S, Anai H, Kabashima N, Kanegae K, Ota T, Tanaka Y, Nakashima Y. 2003. High glucose levels inhibit focal adhesion kinase-mediated wound healing of rat peritoneal mesothelial cells. Kidney Int 63:722–731.

Tanowitz M, Von Zastrow M. 2002. Ubiquitination-independent trafficking of G protein-coupled receptors to lysosomes. J Biol Chem 277:50219–50222.

Tiruppathi C, Song W, Bergenfeldt M, Sass P, Malik AB. 1997. Gp60 activation mediates albumin transcytosis in endothelial cells by tyrosine kinase-dependent pathway. J Biol Chem 272:25968–25975.

Vincent AM, Perrone L, Sullivan KA, Backus C, Sastry AM, Lastoskie C, Feldman EL. 2007. Receptor for advanced glycation end products activation injures primary sensory neurons via oxidative stress. Endocrinology 148:548–558.

Yang D, Chen Q, Yang H, Tracey KJ, Bustin M, Oppenheim JJ. 2007. High mobility group box-1 protein induces the migration and activation of human dendritic cells and acts as an alarmin. J Leukoc Biol 81:59–66.

Zhao YL, Takagawa K, Oya T, Yang HF, Gao Z, Kawaguchi M, Ishii Y, Sasaoka T, Owada K, Furuta I, Sasahara M. 2003. Active Src expression is induced after rat peripheral nerve injury. Glia 42:184–193.

Zochodne DW, Guo GF, Magnowski B, Bangash M. 2007. Regenerative failure of diabetic nerves bridging transection injuries. Diabetes Metab Res Rev 23:490–496.

Zurzolo C, Lisanti MP, Caras IW, Nitsch L, Rodriguez-Boulan E. 1993. Glycosylphosphatidylinositol-anchored proteins are preferentially targeted to the basolateral surface in Fischer rat thyroid epithelial cells. J Cell Biol 121:1031–1039.